

STRONG INFLUENCE OF THE GALACTIC MAGNETIC FIELD ON THE PROPAGATION OF ULTRA-HIGH ENERGY COSMIC RAYS

JIHYUN KIM¹, HANG BAE KIM², AND DONGSU RYU¹

¹Department of Physics, Ulsan National Institute of Science and Technology, Ulsan 689-798, Korea

²Department of Physics and The Research Institute of Natural Science, Hanyang University, Seoul 133-791, Korea

E-mail: jihyunkim@unist.ac.kr, ryu@sirius.unist.ac.kr

(Received November 30, 2014; Revised May 31, 2015; Accepted June 30, 2015)

ABSTRACT

The galactic magnetic field (GMF) and the intergalactic magnetic field (IGMF) affect the propagation of ultra-high energy cosmic rays (UHECRs) from the source to us. Here we examine the influences of the GMF/IGMF and the dependence of their sky distribution on galactic latitude, b . We analyze the correlation between the arrival direction (AD) of UHECRs observed by the Pierre Auger Observatory and the large-scale structure of the universe in regions of sky divided by b . Specifically, we compare the AD distribution of observed UHECRs to that of mock UHECRs generated from a source model constructed with active galactic nuclei. Our source model has the smearing angle as a free parameter that reflects the deflection angle of UHECRs from the source. The results show that larger smearing angles are required for the observed distribution of UHECRs in lower galactic latitude regions. We obtain, for instance, a 1σ credible interval for smearing angle of $0^\circ \leq \theta_s \leq 72^\circ$ at high galactic latitudes, $60^\circ < |b| \leq 90^\circ$, and of $75^\circ \leq \theta_s \leq 180^\circ$, $-30^\circ \leq b \leq 30^\circ$, at low galactic latitudes, respectively. The results show that the influence of the GMF is stronger than that of the IGMF. In addition, we can estimate the strength of GMFs by these values; if we assume that UHECRs would have heavier nuclei, the estimated strengths of GMF are consistent with the observational value of a few μG . More data from the future experiments may make UHECR astronomy possible.

Key words: astroparticle physics — cosmic rays — magnetic fields — methods: statistical

1. INTRODUCTION

The ultra-high energy cosmic rays (UHECRs) are cosmic rays with energies above 10^{19} eV. The flux of UHECRs falls off dramatically at this extremely high energy due to the interactions of UHECRs with cosmic microwave background (CMB) photons. The integrated flux at this energy is about one particle per square kilometer per year. Therefore, direct detection, such as via a balloon-borne detector, is no longer valid; indirect observation using the atmosphere as a huge detector makes it possible to detect the primary particles of UHECRs. To increase the possibility of observation, gigantic ground experiments have been constructed over last 20 years. Despite these efforts, we have still problems to solve in this area. The mass composition and the sources of UHECRs are the main properties of interest. A summary of what we know from recent observational data of UHECRs follows. The mass composition of UHECRs is not conclusive. In chronological order, the High Resolution Fly's Eye experiment (HiRes) claimed that the primary particles seemed to be protons (Abbasi et al., 2009); however, the Pierre Auger Observatory (PAO) reported that the primaries would be heavy nuclei rather

than lighter ones (Abraham et al., 2010). After that, the most recent results from the Telescope Array experiment (TA) (Tinyakov, 2014) show that the primary particles seem to be protons, again.

There have been many studies on the sources of UHECRs. Based on the Greisen-Zatsepin-Kuzmin (GZK) suppression (Greisen, 1966; Zatsepin & Kuzmin, 1966); the steep suppression of the spectrum above the energies $\sim 4 \times 10^{19}$ eV caused by the interaction of UHECRs with CMB photons; we can restrict candidates for the sources; they would be located within $r_{\text{GZK}} \sim 100$ Mpc. There have been many attempts to identify the source of UHECRs using correlation tests with astrophysical objects or the matter distribution in the universe (Abbasi et al., 2008; Abreu et al., 2010; Kim & Kim, 2013; Kashti & Waxman, 2008; Takami et al., 2009); however, we have no conclusive correlation results yet.

When we study the sources of UHECRs, we should consider that the trajectories of UHECRs would be influenced by the intervening magnetic fields while they propagate through the universe, because the primary UHECR is a charged particle. Once we pin down a specific source candidate, we can estimate the properties of the intervening magnetic fields by investigating the deviation from the sources.

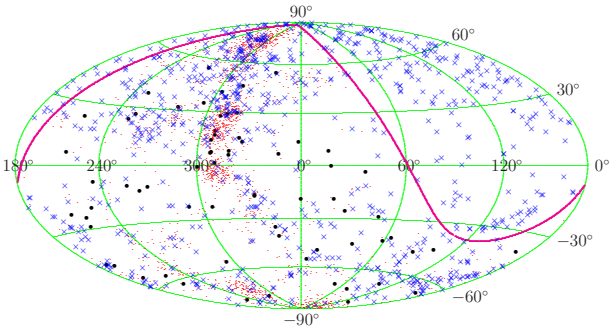


Figure 1. Hammer projections for the skymap in galactic coordinates. The AGN positions (blue), the observed UHECR (black), and the mock UHECR (red) are shown. The magenta line represents the boundary of the field of view for PAO.

There has been much research on the deflection of UHECRs by the galactic magnetic field (GMF) and the intergalactic magnetic fields (IGMF) (Stanev, 1997; Kachelriess et al., 2007; Takami & Sato, 2010; Sigl et al., 2004; Dolag et al., 2005; Ryu et al., 2009; Giacinti et al., 2010, 2011). However, the results are highly model dependent. Therefore, we do not adopt any specific model but adopt the facts that the GMF and IGMF are not uniform; the deflection angles of UHECRs differ from the arrival directions (ADs) in the sky.

In this work, to verify the influence of the GMF/IGMF on the propagation of UHECRs, we will investigate the galactic latitude dependence of the correlation between the ADs of UHECR events and the large scale structure (LSS) of the universe. We divide the sky into three regions in which we are interested, according to galactic latitude.

2. SIMULATION MODEL AND REGIONS OF SKY

To investigate the influence of the GMF/IGMF on the AD of UHECRs, we search for a correlation with the LSS of the universe by comparing an AD distribution of observed UHECR events with that of mock UHECRs by statistical methods.

We assume that the UHECR flux of the source model use to generate mock UHECRs can be written as follows:

$$F(\hat{\mathbf{r}}) \propto \sum_{j \in \text{source}} \frac{1}{4\pi d_j^2} \cdot \exp \left[-(\theta_j(\hat{\mathbf{r}})/\theta_{sj})^2 \right], \quad (1)$$

where $\theta_j(\hat{\mathbf{r}}) = \arccos(\hat{\mathbf{r}} \cdot \hat{\mathbf{r}}'_j)$ is the angle between the direction $\hat{\mathbf{r}}$ and the j -th source $\hat{\mathbf{r}}'_j$, and θ_{sj} is the smearing angle of the j -th source. The second part of this equation, the Gaussian smearing angle, is a free parameter, which reflects the deflection angle of UHECRs from sources by the GMF/IGMF.

Also, we consider the geometrical relative exposure which depends on the AD of UHECR events in equatorial coordinates (Sommers, 2001).

$$h(\delta) = \frac{1}{\pi} [\sin \alpha_m \cos \lambda \cos \delta + \alpha_m \sin \lambda \sin \delta], \quad (2)$$

where δ is the declination of UHECR, λ is the latitude of the detector array, θ_m is the zenith angle cut, and

$$\alpha_m = \begin{cases} 0, & \text{for } \xi > 1, \\ \pi, & \text{for } \xi < -1, \\ \cos^{-1} \xi, & \text{otherwise} \end{cases} \quad \text{with} \quad \xi = \frac{\cos \theta_m - \sin \lambda \sin \delta}{\cos \lambda \cos \delta}. \quad (3)$$

As we can see, the geometrical relative exposure depends on the properties of the observations.

The latitude of the PAO site is $\lambda = -35.2^\circ$ and their zenith angle cut is $\theta_m = 60^\circ$. Thus, the field of view for PAO is $-90^\circ \leq \delta \leq 24.8^\circ$ by Equation (3). In this field of view, the PAO observed 69 UHECR events having energies above 5.5×10^{19} eV (Abreu et al., 2010). We use this data set for observed UHECR events. For a representative of the LSS of the universe, we use active galactic nuclei (AGN) in the 13th edition of Véron-Cetty and Véron catalog (Véron-Cetty & Véron, 2010). There is extensive AGN data in the catalog; however, we only take 600 AGNs located within 100 Mpc taking into account the GZK suppression. Then, we randomly generate mock UHECR events around the positions of AGN using the smearing angle as a standard deviation of the Gaussian distribution by Equation (1). As an example, Figure 1 shows the distributions of observed UHECRs, mock UHECRs, and AGN in galactic coordinates.

The smearing angle in our simulation can be interpreted as a deflection angle from the source by the influence of the intervening magnetic field. When UHECRs propagate from the source to Earth, they experience the force of the GMF and IGMF. Therefore, we need to consider the influence of the GMF/IGMF on the propagation of UHECRs simultaneously.

Unfortunately, the IGMF is less well known than the GMF. Therefore, there are controversies about the deflection angle of UHECRs by the IGMF. For example, Dolag et al. expected that the deflection angle of a proton by the IGMF would be about a few degrees (Dolag et al., 2005). On the other hand, Ryu et al. (2009) estimated quite large deflection angles with a mean value of $\sim 15^\circ$ for protons.

Therefore, we establish a criterion to distinguish the influence of the GMF/IGMF on the propagation of UHECRs instead of adopting any specific model. We divide the regions of sky by the galactic latitude, b , in galactic coordinates. Since the distribution of the IGMF is correlated with the LSS of the universe (Ryu et al., 2008), the galactic latitude dependence of the correlation may give us a basis for distinguishing the influence of the GMF/IGMF. If the influence of the GMF is stronger than that of the IGMF, the deflection angle would be likely to depend on the region of the sky.

In this work, we divide the whole sky into three regions in galactic coordinates. The high galactic latitude region (HGL) covers $60^\circ < |b| \leq 90^\circ$ which includes the galactic poles. The low galactic latitude region (LGL) covers $-30^\circ \leq b \leq 30^\circ$ which contains the galactic plane. The intermediate galactic latitude region

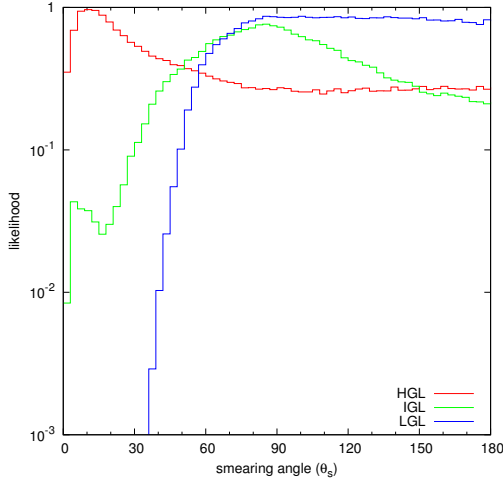


Figure 2. Likelihood dependencies of PAO on the smearing angle (θ_s) using the CADD method. The color lines represent the probabilities for HGL (red), IGL (green), and LGL (blue).

(IGL) covers in-between regions, $30^\circ < |b| \leq 60^\circ$. The properties of each region of sky are summarized in Table 1.

3. STATISTICAL TEST METHOD

In each region, we analyze the correlation between the AD of UHECRs and the LSS of the universe by varying the smearing angle parameter. For the correlation test, we need to extract the characteristics of the AD distribution. We apply a correlational angular distance distribution (CADD), which is the distribution of angular distances between the ADs of UHECRs and those of all sources:

$$\{\cos \theta_{ij'} \equiv \hat{\mathbf{r}}_i \cdot \hat{\mathbf{r}}_{j'} \mid i = 1, \dots, N; j = 1, \dots, M\}, \quad (4)$$

where $\hat{\mathbf{r}}_i$ are the ADs of UHECR, $\hat{\mathbf{r}}_{j'}$ are the point source directions, and N and M are their total numbers, respectively. The CADD is continuous; therefore, we can avoid the loss of information by binning methods, like the cross-correlation function.

To analyze the characteristics obtained by the CADD quantitatively, we compare the CADD from observation to the CADD from simulation using the Kuiper test. The Kuiper statistic, D_{KP} , is defined as follows:

$$D_{KP} = \max_x [S_O(x) - S_E(x)] + \max_x [S_E(x) - S_O(x)], \quad (5)$$

where $S_O(x)$ and $S_E(x)$ are cumulative probability distribution (CPD) of CADD for observation and CPD of CADD for expectation from the source model. The Kuiper statistic is a variant form of the Kolmogorov-Smirnov (KS) statistic. The KS test is a well-known hypothesis test method, but we apply the Kuiper test because it is as sensitive in the tails as at the median of CPDs. Therefore, we can obtain the probability that two different distributions come from the same population through the Monte-Carlo simulation.

4. RESULTS

The results obtained by iterating the correlation test and varying the smearing angle parameter from 0° to 180° at intervals of 3° in each region of sky are shown in Figure 2.

By parameter estimation, we have the smearing angle ranges at the 1σ level in the credible interval: $0^\circ \leq \theta_s \leq 72^\circ$ for HGL, $45^\circ \leq \theta_s \leq 138^\circ$ for IGL, and $75^\circ \leq \theta_s \leq 180^\circ$ for LGL. The lower and upper bounds of smearing angles AT THE 1σ level in the credible interval become larger from the HGL to the IGL.

As mentioned in Section 2, the smearing angle can be interpreted as a deflection angle from the source by the influence of the GMF/IGMF. The results show that the deflection is strongly dependent on galactic latitude. From this, we can conclude that the influence of the GMF is stronger than that of the IGMF on the propagation of UHECRs. Also, we can deduce that the strength of the GMF becomes stronger as the galactic latitude decreases from the trend that the smearing angles become larger.

5. DISCUSSION

To investigate the influence of intervening magnetic field on the AD of UHECRs, we determined the galactic latitude dependence of the correlation with the LSS of the universe in certain regions of sky. We characterized the AD distribution of UHECRs relative to the LSS of the universe by using CADD, then applied the Kuiper test to the source models by varying the smearing angle. By parameter estimation of the smearing angle, we concluded that the influence of the GMF is stronger than that of the IGMF and the strength of the GMF becomes stronger from the HGL to IGL.

From the mid-point value of 1σ level for the smearing angles interval, we can estimate the strength of the GMF. The GMF has a regular field and turbulent field. Observationally, the strength of the turbulent field is $B_{\text{tur}} = (1 - 3)B_{\text{reg}}$; however, the coherence length is much smaller than the traveling distance of the primary particle of UHECRs. Therefore, the deflection by the regular field becomes dominant when the primary of UHECRs propagate through the GMF. Then, we can estimate the strength of the regular GMF by using Equation (6).

$$B_{\text{reg}}[\mu G] \simeq \frac{1}{Z} \frac{\theta_s}{0.57^\circ} \left(\frac{1 \text{ kpc}}{D} \right) \left(\frac{E}{10^{20} \text{ eV}} \right), \quad (6)$$

where Z is the atomic number of the primary particle, B is the strength of the GMF, and D is the distance that the particle passes through.

According to Abraham et al. (2010), the measurements of shower maxima imply that primary particles are presumed to be heavy nuclei. Because we use their data, we assume the iron nuclei having energies above 5.5×10^{19} eV propagate through the of GMF for 1 kpc. Under these conditions, the strength of GMF would be $\gtrsim 1.3 \mu G$, $\gtrsim 3.4 \mu G$, and $\gtrsim 4.7 \mu G$ in HGL, IGL, and

Table 1
CRITERIA OF REGIONS OF SKY, THE PROPERTIES OF EACH REGION, AND THE 1σ CREDIBLE INTERVAL FOR SMEARING ANGLE.

	HGL	IGL	LGL
coverage	$60^\circ < b \leq 90^\circ$	$30^\circ < b \leq 60^\circ$	$-30^\circ \leq b \leq 30^\circ$
# of AGN	163	271	166
# of PAO	8	22	39
1σ C.I.	$0^\circ \leq \theta_s \leq 72^\circ$	$45^\circ \leq \theta_s \leq 138^\circ$	$75^\circ \leq \theta_s \leq 180^\circ$

LGL by using Equations (6), respectively. These values are consistent with observational values (Beck, 2001).

More data from the future experiments make it possible to study the GMF between the source of UHECRs and Earth more accurately. UHECR astronomy may be feasible in the near future.

ACKNOWLEDGMENTS

The work was supported by the National Research Foundation of Korea through grant 2007-0093860 and 2012R1A1A2008381.

REFERENCES

- Abbasi, R. U., et al., 2008, Search for Correlations Between HiRes Stereo Events and Active Galactic Nuclei, *APh*, 30, 175
- Abbasi, R. U., et al., 2010, Indications of Proton-Dominated Cosmic-Ray Composition above 1.6 EeV, *PhRvL*, 104, 1101
- Abraham, J., et al., 2010, Measurement of the Depth of Maximum of Extensive Air Showers above 10^{18} eV, *PhRvL* 104, 1101A
- Abreu, P., et al., 2010, Update on the Correlation of the Highest Energy Cosmic Rays with Nearby Extragalactic Matter, *APh*, 34, 314
- Beck, R., 2001, Galactic and Extragalactic Magnetic Fields, *SSRv*. 99, 243
- Dolag, K., et al., 2005, Constrained Simulations of the Magnetic Field in the Local Universe and the Propagation of Ultrahigh Energy Cosmic Rays, *JCAP* 1, 37
- Giacinti, G., et al., 2010, Ultrahigh Energy Nuclei in the Galactic Magnetic Field, *JCAP* 8, 17
- Giacinti, G., et al., 2011, Ultrahigh Energy Nuclei in the Turbulent Galactic Magnetic Field, *APh*, 35, 192
- Greisen, K., 1966, End to the Cosmic Ray Spectrum?, *PhRvL*, 16, 748
- Kachelriess, M., et al., 2007, The Galactic Magnetic Field as Spectrograph for Ultra-high Energy Cosmic Rays, *Aph*, 26, 378
- Kashti, T. & Waxman, E., 2008, Searching for a Correlation between Cosmic-ray Sources above 10^{19} eV and Large Scale Structure, *JCAP*, 5, 6
- Kim, H. B. & Kim, J., 2013, Revisit of Correlation Analysis between Active Galactic Nuclei and Ultra-High Energy Cosmic Rays, *IJMPD*, 22, 21
- Ryu, D., et al., 2008, Turbulence and Magnetic Fields in the Large-scale Structure of the Universe, *Science*, 320, 909
- Ryu, D., et al., 2010, Intergalactic Magnetic Field and Arrival Direction of Ultra-High-Energy Protons, *ApJ*, 710, 1422
- Sigl, G., et al., 2004, Ultrahigh Energy Cosmic Ray Probes of Large Scale Structure and Magnetic Fields, *PhRvD* 70, 16
- Sommers, P., 2001, Cosmic Ray Anisotropy Analysis with a Full-sky Observatory, *AP*, 14, 271
- Stanev, T., 1997, Ultra-high-energy Cosmic Rays and the Large-scale Structure of the Galactic Magnetic Field, *ApJ*, 479, 290
- Takami, H., et al., 2009, Cross-correlation between UHECR Arrival Distribution and Large-scale Structure, *JCAP*, 6, 19
- Takami, H. & Sato, K., 2010, Does Galactic Magnetic Field Disturb the Correlation of the Highest Energy Cosmic Rays with their Sources?, *ApJ* 724, 1456
- Tinyakov, P. & Telescope Array Collaboration 2014, Latest Results from the Telescope Array, *NIMPA*, 742, 29
- Véron-Cetty, M. P. & Véron, P., 2010, A Catalogue of Quasars and Active Nuclei: 13th Edition, *A&A* 518, 8
- Zatsepin, G.T. & Kuzmin, V. A., 1966, Upper Limit of the Spectrum of Cosmic Rays, *JETPL*, 4, 78